

# Chromosomal organization and fluorescence *in situ* hybridization of the human Sirtuin 6 gene

ULRICH MAHLKNECHT<sup>1</sup>, ANTHONY D. HO<sup>1</sup> and SUSANNE VOELTER-MAHLKNECHT<sup>2</sup>

<sup>1</sup>Department of Hematology/Oncology, University of Heidelberg Medical Center, Im Neuenheimer Feld 410, D-69120 Heidelberg; <sup>2</sup>Department of Occupational, Social and Environmental Medicine, University of Mainz, Obere Zahlbacher Str. 67, D-55131 Mainz, Germany

Received August 17, 2005; Accepted October 21, 2005

**Abstract.** Sirtuin 6 (SIRT6) is a member of the sirtuin deacetylases (sirtuins), which are derivatives of the yeast Silent information regulator 2 (Sir2) protein. SIR2 and its mammalian derivatives play a central role in epigenetic gene silencing, recombination, metabolism, cell differentiation and in the regulation of aging. In contrast to most sirtuins, SIRT6 lacks NAD<sup>+</sup>-dependent protein deacetylase activity. We have isolated and characterized the human *Sirt6* genomic sequence, which spans a region of 8,427 bp and which has one single genomic locus. Determination of the exon-intron splice junctions found the full-length SIRT6 protein to consist of 8 exons ranging in size from 60 bp (exon 4) to 838 bp (exon 8). The human *Sirt6* open reading frame encodes a 355-aa protein with a predictive molecular weight of 39.1 kDa and an isoelectric point of 9.12. Characterization of the 5' flanking genomic region, which precedes the *Sirt6* open reading frame, revealed a TATA- and CCAAT-box less promoter with an approximately 300-bp long CpG island. A number of AML-1 and GATA-x transcription factor binding sites were found which remain to be further evaluated experimentally. Fluorescence *in situ* hybridization analysis localized the human *Sirt6* gene to chromosome 19p13.3; a region which is frequently affected by chromosomal alterations in acute leukemia. Human SIRT6 appears to be most predominantly expressed in bone cells and in the ovaries while, in the bone marrow, it is practically absent. The functional characteristics of SIRT6 are essentially unknown at present and remain to be elucidated.

## Introduction

Based on structural and functional similarities, mammalian histone deacetylases are grouped into four categories, of which three contain non-sirtuin HDACs comprising the yeast histone deacetylases, RPD3 (class I HDACs), HDA1 (class II HDACs) and the more recently described HDAC11-related enzymes (class IV HDACs), while one category consists of sirtuin histone deacetylases (class III HDACs), which are homologs to the yeast Sir2 protein. SIRT1 is the mammalian sirtuin that is most closely related to *S. cerevisiae* SIR2. By contrast, mammalian SIRT6 is strongly related to SIRT7 (1) but only distantly homologous to human SIRT1 and yeast SIR2. The currently known seven human sirtuins have been further subgrouped into four distinct phylogenetic classes: SIRT1, SIRT2, and SIRT3 (subclass 1); SIRT4 (subclass 2); SIRT5 (subclass 3); and, finally, SIRT6 and SIRT7 (subclass 4, Fig. 1 and Table I) (1,2). Derivatives of the yeast SIR2 histone deacetylase share a common catalytic domain which is highly conserved in organisms ranging from bacteria to humans and which is composed of two distinct motifs that bind NAD<sup>+</sup> and the acetyl-lysine substrate, respectively (3,4). The yeast silent information regulator 2 protein (SIR2) is a NAD<sup>+</sup>-dependent histone deacetylase, which hydrolyzes one molecule of NAD<sup>+</sup> for every lysine residue that is deacetylated (5). The yeast Sir2 protein, as well as its mammalian derivatives, has been shown to directly modify chromatin and to silence transcription (6-10), to modulate the meiotic checkpoint (11) and, as a probable anti-aging effect, to increase genomic stability and suppress rDNA recombination (8,12,13). While yeast SIR2 exclusively targets histone proteins, mammalian SIRT1 has a large and growing list of targets, such as p53 and forkhead transcription factors, which are mammalian homologs of the Daf-16 protein, a key regulator within the insulin signaling pathway (8,14).

SIRT6 is a broadly expressed protein, which is predominantly found in the cell nucleus. In a tissue distribution analysis in the mouse embryo, SIRT6 reached peak levels at day E11, which further persisted into adulthood in muscle, brain and heart cells (15). The yeast silent information regulator 2 protein (SIR2); its mammalian orthologs, SIRT1, SIRT2, SIRT3, and SIRT5; and the bacterial protein, CobB; catalyze the tightly coupled cleavage of NAD<sup>+</sup> and protein deacetylation, producing nicotinamide and 2-O-acetyl-ADP-

---

*Correspondence to:* Dr U. Mahlknecht, Department of Hematology/Oncology, University of Heidelberg Medical Center, Im Neuenheimer Feld 410, D-69120 Heidelberg, Germany  
E-mail: ulrich.mahlknecht@med.uni-heidelberg.de

*Abbreviations:* HDAC, histone deacetylase; HAT, histone acetyltransferase

*Key words:* sirtuins, histones, chromatin, histone deacetylase, chromosomes, genes, structural

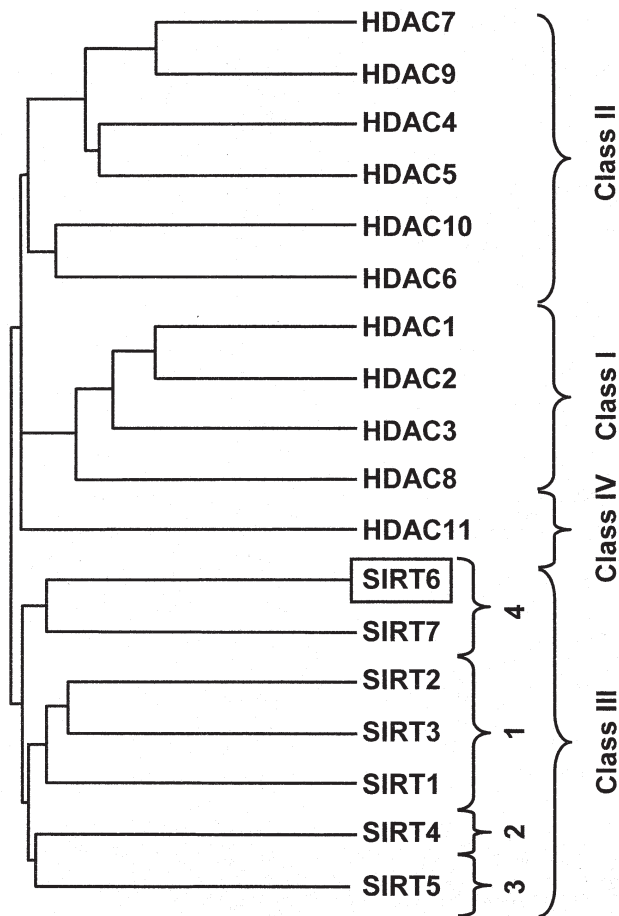


Figure 1. The position of human SIRT6 among the human orthologs for yeast RPD3, HDA1, SIR2 and HDAC11 related protein families of histone deacetylases (HDAC classes I-IV) and within the sirtuin-subclasses (subclasses 1-4) is shown (accession numbers of the sequences used in this tree: human HDAC1 (GenPept Q13547), human HDAC2 (GenPept Q92769), human HDAC3 (GenPept O15379), human HDAC8 (GenPept AAF73428), human HDAC4 (GenPept AAD29046), human HDAC5 (GenPept AAD29047), human HDAC6 (GenPept AAD29048), human HDAC7 (GenPept AAF04254), human HDAC9 (GenPept AAK66821), human HDAC10 (GenPept AAL30513), human HDAC11 (GenPept NP\_079103), human SIRT1 (GenPept AAD40849), human SIRT2 (GenPept NP\_036369), human SIRT3 (GenPept AAD40851), human SIRT4 (GenPept AAD40852), human SIRT5 (GenPept AAD40853), human SIRT6 (GenPept NP\_057623) and human SIRT7 (GenPept AAF43431) (4).

ribose reaction products (16). The deacetylase activity of sirtuin proteins is tightly coupled with their phosphoribosyltransferase activity and requires the presence of highly specific conserved amino-acid residues within the catalytic core of the protein, which are not contained in mammalian SIRT4, SIRT6, or SIRT7 and which are, therefore, lacking enzymatic deacetylase activity (2,8,15,17-19).

Calorie restriction is known to induce a metabolic switch that increases the NAD/NADH ratio and/or decreases levels of nicotinamide, which is a yeast SIR2 inhibitor, and as a result activates SIR2 and increases rDNA stability (8,20). Sirtuins, therefore, create a direct link between cellular energy status and longevity (8,21). Mammalian SIRT1 binds, deacetylates and reduces the activity of several transcription factors *in vivo*, including MyoD, p53, and FOXO, thereby affecting cell differentiation and survival under stress (14,22,23). The effect of SIRT1 on p53 may be inhibited by Nicotinamide (vitamin B3) (23-25). Calorie restriction in mammalian cells activates FOXO3A and increases FOXO3A-mediated expression of SIRT1, which depends on the presence of two p53 binding sites in the SIRT1 promoter, and a nutrient-sensitive physical interaction that was observed between FOXO3A and p53 (14,26,27).

A cell that is low in energy will consume most of its NADH to generate ATP. The consequential high levels of nicotinamide adenine dinucleotide (NAD<sup>+</sup>) provide the indispensable cosubstrate for SIR2, which then activates acetyl-CoA synthetase (ACS) and subsequently results in the generation of more acetyl CoA, thus shunting more carbon into the NADH- and energy-generating TCA cycle (28). In addition to the generation of acetyl CoA, active Sir2 is also known to extend lifespan. More acetyl CoA for the citric acid cycle means more respiration, which has been associated with yeast lifespan extension when caloric intake is restricted. Accordingly, when mammals are short of food they also alter their metabolism such that both aging and reproduction are postponed until better times (28).

In contrast to SIRT1, only minimal information is currently available on human SIRT6, which is a distantly related ortholog of yeast SIR2 (1,29), and which has been predicted to be predominantly a nuclear protein (78.3% nuclear, 13.0% cyto-

Table I. Sequence identity and similarity among human class III sirtuin proteins.<sup>a</sup>

	Human SIRT1	Human SIRT2	Human SIRT3	Human SIRT4	Human SIRT5	Human SIRT6	Human SIRT7	Yeast SIR2
Human SIRT1		42	40	30	28	22	23	40
Human SIRT2	65		50	26	27	27	25	31
Human SIRT3	63	66		28	31	28	28	35
Human SIRT4	47	43	43		27	28	28	25
Human SIRT5	43	44	43	46		21	24	26
Human SIRT6	39	44	40	43	36		42	23
Human SIRT7	39	42	40	45	37	56		21
Yeast SIR2	56	47	49	44	41	38	38	

<sup>a</sup>The indicated numbers represent the percentage of sequence identity and similarity from pairwise sequence comparisons.





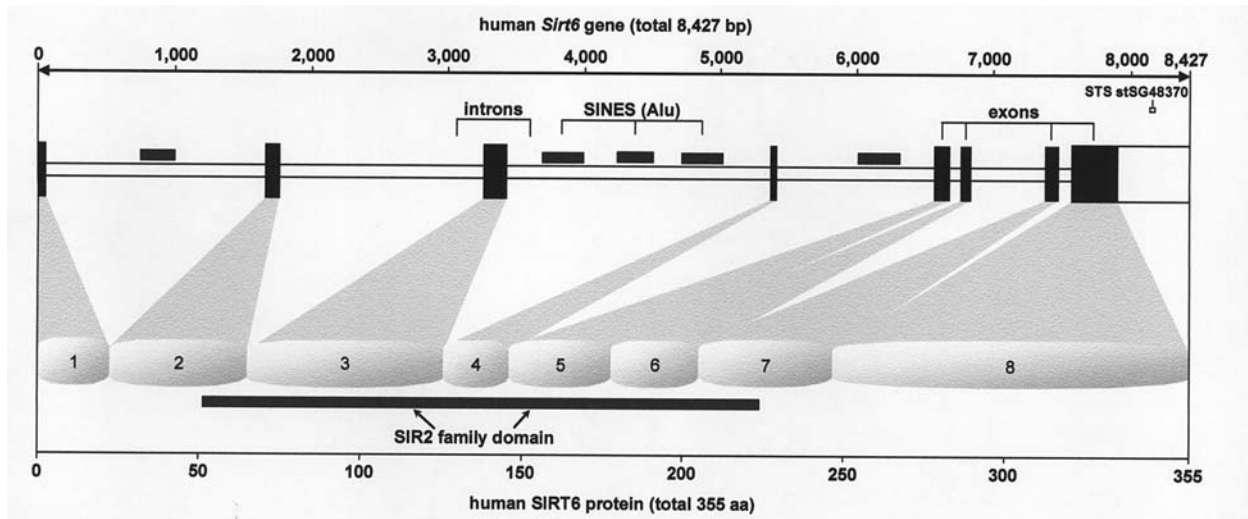


Figure 3. Genomic organization of the human *Sirt6* gene. The genomic organization of the 8,427-bp long *Sirt6* gene, which includes the relative position of exons and introns, is shown. Repetitive sequences, known as short interspersed nuclear elements (SINES) are indicated. The position of internal STS-marker, stSG48370, is indicated. The sirtuin catalytic domain overlaps the SIRT6 protein region that is encoded by exons 2 through 7.

as a modulator of endocrine changes. In the study presented herein, we report the chromosomal localization and genomic organization of the human *Sirt6* gene.

#### Materials and methods

**Identification of the human *Sirt6* cDNA.** A homology search of the EST database at NCBI (National Center for Biotechnology Information) with the human *Sirt6* cDNA that has been published earlier (1) yielded 7 positive cDNA clones of which one was obtained from the Reference Center of the German Human Genome Project (RZPD, Berlin, Germany). The authenticity of their inserts was confirmed by DNA cycle sequencing (Fig. 2).

**Identification of BAC genomic clone, RZPDB737G031026D6.** The human *Sirt6* genomic clone was obtained from an arrayed BAC genomic library (Human Genomic Set - RZPD 1.0) after *in silico* screening with *Sirt6* cDNA (GenBank clone NM\_016539), which was shown to contain full-length human *Sirt6* cDNA. BAC clone, RZPDB737G031026D6, was identified to contain inserts with an average size of approximately 120 kb in the vector, pBACe3.6, which included the human *Sirt6* genomic sequence. BAC genomic DNA was prepared according to published protocols (31) and the *Sirt6* insert was confirmed by cycle sequencing (32).

**Instrumental methods.** Dye terminator cycle sequencing was performed using the ABI PRISM™ BigDye Terminator Cycle Sequencing Ready Reaction Kit with AmpliTaq™ DNA polymerase (Perkin-Elmer, Branchburg, NJ) and analyzed using an ABI PRISM 310 Genetic Analyzer which utilizes the four-color sequencing chemistry.

**PCR methods.** The human *Sirt6* sequence was partially sequenced by primer walking on both strands using a direct sequencing strategy (32). Sequencing reactions were performed using 0.6  $\mu$ g cDNA and 20-30mer oligonucleotide primers

(Thermo Electron, Dreieich, Germany). Sequencing reactions were set up in a volume of 20  $\mu$ l containing 10 pmol of the sequencing primer, 4  $\mu$ l BigDye Terminator Cycle Sequencing Ready Reaction Mix (Perkin-Elmer, Norwalk, CT), and DNA as indicated, and ddH<sub>2</sub>O was added to a final volume of 20  $\mu$ l. The thermal cycling profile for the sequencing of the cDNA-clones was as follows: denaturation at 95°C for 30 sec, annealing at 50°C for 15 sec, extension at 60°C for 4 min (25 cycles), and storage at 4°C.

***Sirt6* chromosomal localization by fluorescence in situ hybridization (FISH).** Standard chromosome preparations were used from a human lymphoblastoid cell line. In order to remove excess cytoplasm, slides were treated with pepsin (0.5 mg/ml in 0.01 M HCl, pH 2.0) at 37°C for 40 min. Slides were then washed for 2x10 min in 1X PBS and 1x10 min in 1X PBS/50 mM MgCl<sub>2</sub> at room temperature. BAC DNA was labeled by using a standard nick translation procedure. Digoxigenin (Roche Diagnostics) was used as labeled dUTP at the concentration of 40  $\mu$ M. Probe length was analyzed on a 1% agarose gel. The probe showed an optimal average length of ~300 bp after nick translation. Approximately 50 ng DNA were pooled with 2  $\mu$ g cot-1 in 10  $\mu$ l hybridization buffer (50% formamide, 2X SSC, 10% dextran sulfate). The DNA was applied to chromosomes fixed on a slide, mounted with a cover slip and sealed with rubber cement. Probe DNA and chromosomes were denatured at 72°C for 3 min. Hybridization was overnight at 37°C in a wet chamber. After hybridization, the cover slip was carefully removed and the slide was washed in 2X SSC for 8 min. The slide was then incubated at 72°C in 0.4X SSC/0.1% Tween for 1 min, washed shortly in 2X SSC at room temperature, and stained in DAPI (4',6-diamidino-2-phenylindole) for 10 min. For microscopy, the slide was mounted in antifade solution (Vectashield). *In situ* hybridization signals were analyzed on a Zeiss Axioplan II microscope. Each image plain (blue and orange) was recorded separately with a b/w CCD camera. Chromosomes and FISH signals were then displayed in false colors

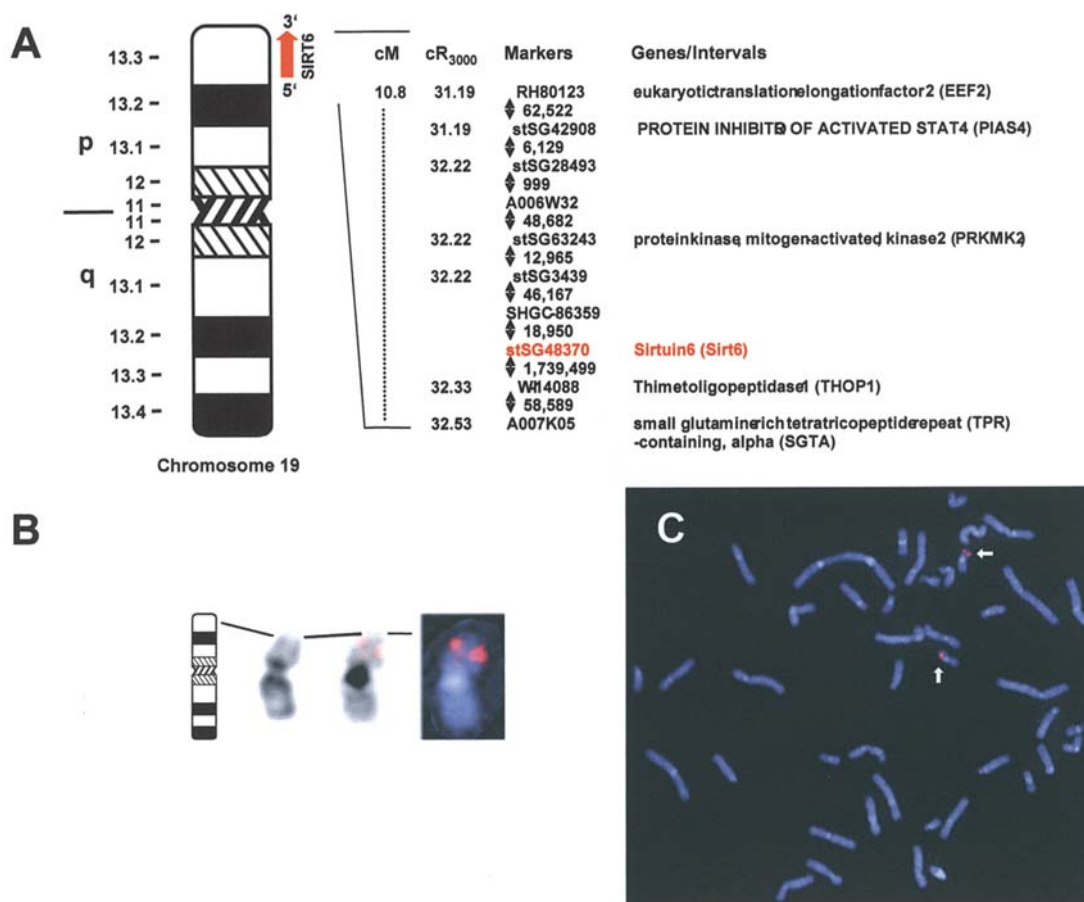


Figure 4. Chromosomal mapping of the human *Sirt6* gene. Upper panel (A), chromosome 19 ideogram according to the International System for Cytogenetic Nomenclature (ISCN 1995). The chromosomal position of BAC clone *RZPDB737G031026D6* in close proximity to the *PRKMK2* gene (located telomerically) and the *THOP1* gene (located centromerically) is shown as well as the chromosomal orientation of *Sirt6* gene (red arrow). (B) From left to right, next to the chromosome 19 ideogram, pictures of a DAPI-stained chromosome 19, together with the same chromosome carrying the BAC hybridization signal, are illustrated. (C) Fluorescence *in situ* hybridization of BAC clone *RZPDB737G031026D6* to human chromosome 19p13.3.

and images merged on the computer. Camera control, image capture and merging were performed using SmartCapture X software (Digital Scientific, Cambridge, UK) (Fig. 4).

**Sequence analysis and computer database searches.** DNA sequence analysis was performed using the HUSAR (Heidelberg Unix Sequence Analysis Resources) server hosted by the Biocomputing Service Group at the German Cancer Research Center (DKFZ, Heidelberg) and the UniGene and LocusLink programs at the National Center for Biotechnology Information (NCBI). Sequence comparisons were performed using the BLAST algorithm of the GenBank and EMBL databases (33). Protein similarity scores were calculated from fast alignments generated by the method of Wilbur and Lipman using the CLUSTAL W Multiple Alignment Program Version 1.7 (Figs. 1 and 5; Tables I and III) (34). Protein motifs were identified online at the ExpASY (Expert Protein Analysis System) proteomics server of the Swiss Institute of Bioinformatics (SIB) with the program, PROSITE, and double-checked using the MotifFinder program hosted by the GenomeNet server at the Bioinformatics Center at the Institute for Chemical Research from the Kyoto University (Japan). Potential transcription factor binding sites were identified using the TRANSFAC program, which is part of the GenomeNet Computation Service (see above), but remain

to be confirmed experimentally. Sequence similarities were calculated using GAP software, which considers all possible alignments and gap positions between two sequences and creates a global alignment that maximizes the number of matched residues and minimizes the number and size of gaps on the HUSAR server (35). Repetitive and CpG elements were identified on the RepeatMasker Server and with the CPG software hosted by the European Bioinformatics Institute (EMBL outstation) (Figs. 2 and 3).

**Phylogenetic analysis.** Phylogenetic trees were constructed from known human class I through class IV histone deacetylase sequences which were obtained from protein sequence similarity searches with the yeast proteins, RPD3, HDA1 and SIR2, using the BLAST 2.0 program at NCBI database (Non-redundant GenBank CDS: translations+PDB+SwissProt +SPupdate+PIR). Progressive multiple sequence alignments were performed using the CLUSTAL W Multiple Alignment Program Version 1.7 (Fig. 1) (4,36). Trees were then calculated and drawn using PileUp software, which computes a multiple sequence alignment using a simplification of the progressive alignment method of Feng and Doolittle (37) and which can plot a dendrogram like the one below, that shows the clustering relationships used to determine the order of the pairwise alignments that together create the final multiple sequence

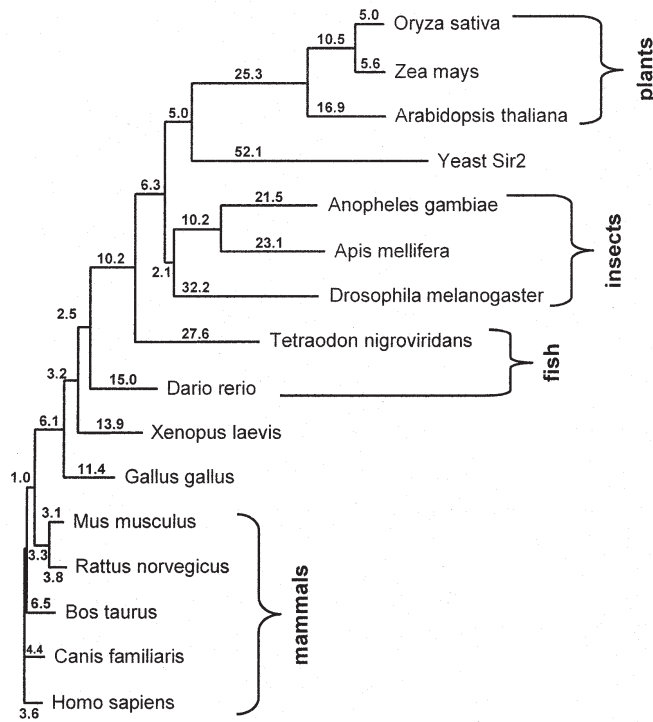


Figure 5. SIRT6 phylogenetic tree. This dendrogram depicts the sequence relatedness of the human SIRT6 protein with the SIRT6 homologs from different species. The GenPept accession numbers correspond to the ones that have also been used for the multiple sequence alignment as shown in Table III.

alignment. Distance along the vertical axis is proportional to the difference between sequences; distance along the horizontal axis has no significance at all. Trees in Fig. 5 were calculated and drawn using PATH (Phylogenetic Analysis Task in HUSAR) software, which estimates and realizes phylogenies by executing the three main phylogenetic methods: distance, parsimony and maximum likelihood, and which is hosted by the HUSAR (Heidelberg Unix Sequence Analysis Resources) server from the Biocomputing Service Group at the German Cancer Research Center (DKFZ, Heidelberg).

**Results**

Identification and cloning of cDNAs encoding human Sirt6. Homology searches of the dbEST at NCBI (National Center for Biotechnology Information) (33) for the *Sir6* cDNA sequence (1,2) yielded 7 positive cDNA clones: GenBank NM\_016539 (1,638 bp), AF233396 (1,638 bp), AK074810 (1,603 bp), BC004218 (1,398 bp), BC005026 (1,600 bp), BC028220 (1,585 bp) and CR457200 (1,068 bp), of which GenBank clone NM\_016539 was obtained from the Reference Center of the German Human Genome Project (RZPD, Berlin, Germany). The authenticity of its insert was confirmed by DNA cycle sequencing (Fig. 2). Sequences flanking the 5' and 3' ends of the Sirt6 open reading frame were identified from the *Sirt6* human genomic clone, BAC RZPDB737G031026D6. The human *Sirt6* mRNA is transcribed into a 1,638-bp mRNA with an open reading frame of 1,065 bp, which is translated into a 355-aa protein with a predictive molecular weight of 39.1 kDa and an isoelectric point of 9.12. Characterization of the 5' flanking genomic region, which precedes the *Sirt6* open reading frame, revealed a TATA- and CCAAT-box less promoter with an approximately 300-bp CpG island. A number of GATA-x and AML-1 transcription factor binding sites were found which remain to be further evaluated experimentally. Fluorescence *in situ* hybridization analysis localized the human *Sirt6* gene to chromosome 19p13.3. Translational stop codons in all reading frames precede the human *Sirt6* open reading frame. The 3' flanking region was shown to contain the eukaryotic polyadenylation consensus signal AATAAA (38), 484 bp downstream of the termination of translation signal TGA (Fig. 2).

*Identification and characterization of the human Sirt6 genomic locus.* The human *Sirt6* genomic clone was obtained from an arrayed BAC genomic library (Human Genomic Set - RZPD 1.0) after *in silico* screening with *Sirt6* cDNA (GenBank clone NM\_016539), which was shown to contain full-length human *Sirt6* cDNA. BAC clone RZPDB737G031026D6 was identified to contain inserts with an average size of approximately 120 kb in the 11.6-kb vector, pBACE3.6, which

Table II. Exon/intron splice-junctions of the human *Sirt6* gene: exon sequences are given in uppercase and intron sequences are given in lowercase letters.<sup>a</sup>

Exon no.	Exon size	5'-splice donor	Intron no.	Intron size	3'-splice acceptor
1	66	CCTCCCGGAG <b>gt</b> gagcgcgtct	1	1.564	ctccccccac <b>ag</b> ATCTTCGACC
2	128	CCGACTTCAG <b>gt</b> ctgtgattgt	2	1.491	tgccaccttc <b>ag</b> GGGTCCCCAC
3	183	GCTTCCCCAG <b>gt</b> aacaccctgg	3	1.965	ctcttcccac <b>ag</b> GGACAAACTG
4	60	AGTGTAAGAC <b>gt</b> gagtgccacc	4	1.141	tccttgacac <b>ag</b> GCAGTACGTC
5	96	GAGCCTGCAG <b>gt</b> gagccacccc	5	81	tcctcattgc <b>ag</b> GGGAGAGCTG
6	81	AGGCCAGCAG <b>gt</b> ctgaccccc	6	528	ccccggcccc <b>ag</b> GAACGCCGAC
7	124	CACCAAGCAC <b>gt</b> taggtgtctga	7	81	gccccccggc <b>ag</b> GACCGCCATG
8	838				

<sup>a</sup>The sizes of the single exons and introns are indicated. Consensus splice donor and splice acceptor sequences are given in bold.



Table III. Amino-acid sequence alignment of the human SIRT6 catalytic domain with SIRT6 homologs from different species.<sup>a</sup>

	11	50	100	150
Anopheles gambiae	--MSCN.YAE	GISKYENK.G	VLGVAE...	I
Apis mellifera	--MSCS.YAD	GLSQYENK.G	VLGLEE...	R
Arabidopsis thaliana	--MSLG.YAE	KLSFIEDV.G	Q'GWMAE	F
Bos taurus	--MSVN.YAA	GLSEYADK.G	KCGLPE...	V
Canis familiaris	--MSVN.YAA	GLSEYADK.G	KCGLPE...	I
Dario rerio	--MSVN.YAA	GLSEYADK.G	KCGLPE...	T
Drosophila melanogaster	--MSCN.YAD	GLSEYADK.G	ILGAPL...	S
Gallus gallus	--MAVR.YAA	GLSEYADK.G	KCGLPE...	I
Homo sapiens	--MSVN.YAA	GLSEYADK.G	KCGLPE...	I
Mus musculus	--MSVN.YAA	GLSEYADK.G	KCGLPE...	I
Oryza sativa	--MSLG.YAE	KLSYREDV.G	NVGMPE...	F
Rattus norvegicus	--MSVN.YAA	GLSEYADK.G	KCGLPE...	I
Tetraodon nigroviridans	--MSVR.YAA	GLSEYADK.G	VCGLPE...	E
Xenopus laevis	--MSVN.YAA	GLSEYADK.G	KCGLPE...	Q
Zea mays	--MSLG.YAE	KLSYREDV.G	TVGNPE...	I
Yeast Sir2	SKTSENKAVN	TVSPQDKA	LRKQDDIN	IRKQDDIN
	151	200	250	300
Anopheles gambiae	IVS...	QNDI	GHILRSQAR	E...
Apis mellifera	IVS...	QNDI	GHILRSQOR	Q...
Arabidopsis thaliana	VIS...	QNVQ	GHILRSQIR	E...
Bos taurus	IVS...	QNVQ	GHVRSQFR	D...
Canis familiaris	IVS...	QNVQ	GHVRSQFR	D...
Dario rerio	LIS...	QNVQ	GHVRSQFR	D...
Drosophila melanogaster	VIS...	QNVQ	GHILRSQDR	K...
Gallus gallus	IVS...	QNVQ	GHVRSQFR	D...
Homo sapiens	IVS...	QNVQ	GHVRSQFR	D...
Mus musculus	IVS...	QNVQ	GHVRSQFR	D...
Oryza sativa	VIS...	QNVQ	SHILRSQDR	E...
Rattus norvegicus	IVS...	QNVQ	GHVRSQFR	D...
Tetraodon nigroviridans	LIS...	QNVQ	GHVRSQFR	D...
Xenopus laevis	IVS...	QNVQ	GHVRSQFR	Z...
Zea mays	VIS...	QNVQ	SHILRSQFR	Z...
Yeast Sir2	LDVTLFEDIN	SKTYVILK	LGFEVDDQK	LGFEVDDQK
	350	400	450	500
Anopheles gambiae	GRGVIC	QK	GRVVIC	QK
Apis mellifera	GRVVIC	QK	GRVVIC	QK
Arabidopsis thaliana	GKIVY	QK	KTPK	QK
Bos taurus	GRVVIC	QK	GRVVIC	QK
Canis familiaris	GRVVIC	QK	GRVVIC	QK
Dario rerio	GKIVY	QK	GRVVIC	QK
Drosophila melanogaster	GRVVIC	QK	GRVVIC	QK
Gallus gallus	GRVVIC	QK	GRVVIC	QK
Homo sapiens	GRVVIC	QK	GRVVIC	QK
Mus musculus	GRVVIC	QK	GRVVIC	QK
Oryza sativa	GRVVIC	QK	GRVVIC	QK
Rattus norvegicus	GRVVIC	QK	GRVVIC	QK
Tetraodon nigroviridans	GKIVY	QK	GRVVIC	QK
Xenopus laevis	GKIVY	QK	GRVVIC	QK
Zea mays	GKIVY	QK	GRVVIC	QK
Yeast Sir2	DDPQVFN	IFM	DPQVFN	IFM
	550	600	650	700
Anopheles gambiae	GRVVIC	QK	GRVVIC	QK
Apis mellifera	GRVVIC	QK	GRVVIC	QK
Arabidopsis thaliana	GKIVY	QK	KTPK	QK
Bos taurus	GRVVIC	QK	GRVVIC	QK
Canis familiaris	GRVVIC	QK	GRVVIC	QK
Dario rerio	GKIVY	QK	GRVVIC	QK
Drosophila melanogaster	GRVVIC	QK	GRVVIC	QK
Gallus gallus	GRVVIC	QK	GRVVIC	QK
Homo sapiens	GRVVIC	QK	GRVVIC	QK
Mus musculus	GRVVIC	QK	GRVVIC	QK
Oryza sativa	GRVVIC	QK	GRVVIC	QK
Rattus norvegicus	GRVVIC	QK	GRVVIC	QK
Tetraodon nigroviridans	GKIVY	QK	GRVVIC	QK
Xenopus laevis	GKIVY	QK	GRVVIC	QK
Zea mays	GKIVY	QK	GRVVIC	QK
Yeast Sir2	DDPQVFN	IFM	DPQVFN	IFM

<sup>a</sup>ClustalW Colors mark similarities in protein sequences. Black background, more than 75% of nucleotides of a column are identical. Grey, more than half of the amino acids of a column are identical or belong to one of the strong groups (amino acids with strong similarities). Accession numbers of the sequences used in this alignment: Anopheles gambiae (GenPept XP\_321669), Apis mellifera (GenPept XP\_396298), Arabidopsis thaliana (GenPept BAB09243), Bos taurus (GenPept XP\_615499), Canis familiaris (GenPept XP\_542163), Dario rerio (zebrafish, GenPept AAH71405), Drosophila melanogaster (GenPept AAF54513), Gallus gallus (GenPept CAG30975), Homo sapiens (GenPept NP\_057623), Mus musculus (GenPept NP\_853617), Oryza sativa (GenPept XP\_471492), Rattus norvegicus (GenPept XP\_234931), Tetraodon nigroviridans (GenPept CAG07749), Xenopus laevis (GenPept AAH72991), Zea mays (GenPept AAK67144), yeast Sir2 (GenPept P06700).

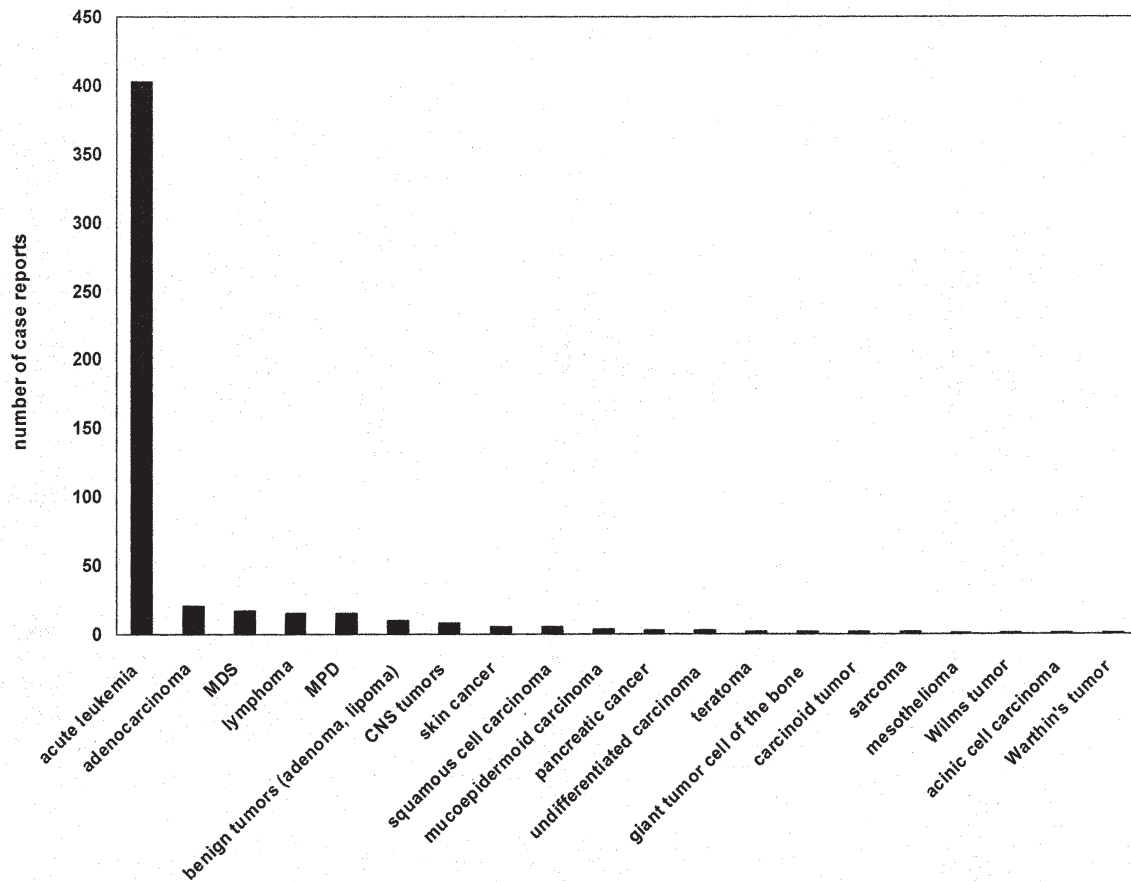


Figure 6. The chromosome region, 19p13, is a section which has been found to be involved in various malignancies. Of 522 case reports, which have been retrieved from the Cancer Genome Anatomy Project (CGAP) database at the National Cancer Institute (45), the most frequent mutations and chromosomal alterations have been found in acute leukemias (403; with 135 AML, 257 ALL, 11 bilineage biphenotypic leukemia), adenocarcinomas (21), MDS (17), lymphoma (15; with 4 CLL, 1 mycosis fungoides, 3 Burkitt lymphoma, 1 Hodgkin's disease, 2 multiple myeloma, 1 T-cell lymphoma, 1 B-cell lymphoma, 2 hairy cell leukemia), myeloproliferative disease (15; with 14 CML, 1 polycythaemia vera), benign tumors (10; with 2 lipoma, 2 papilloma, 2 adenoma, 2 leiomyoma, 1 solitary fibrous tumor, 1 benign epithelial tumor), central nervous system tumors (9; with 7 meningiomas, 1 astrocytoma, 1 primitive neuroectodermal tumor), skin cancer (5; with 4 basal cell carcinoma, 1 dysplastic nevus), 5 squamous cell carcinomas, 4 mucoepidermoid carcinomas, 3 pancreatic cancers, 3 undifferentiated carcinomas, 2 teratomas, 2 giant tumor cell of the bone, 2 carcinosarcomas, 2 sarcomas, 1 mesothelioma, 1 Wilms tumor, 1 acinic cell carcinoma and 1 Warthin's tumor.

included the human *Sirt6* genomic sequence. BAC genomic DNA was prepared according to published protocols (31) and the *Sirt6* insert was confirmed by cycle sequencing (32). Genomic sequence comparison analyses with the BLAST algorithm helped us with the identification of human chromosome 6 genomic contig NT\_011245, which was sequenced and assembled from individual clone sequences by the Human Genome Sequencing Consortium together with NCBI. We have used this sequence for the determination of *Sirt6* introns and exon/intron boundaries (Table II). The human *Sirt6* gene spans a region of 8,427 bp (Fig. 3). Determination of the exon-intron splice junctions found the full-length SIRT6 protein to consist of 8 exons ranging in size from 60 bp (exon 4) to 838 bp (exon 8). Within introns 1, 3 and 4 we identified an accumulation of interspersed repetitive elements, SINEs (short interspersed nuclear elements) (Fig. 3). Additionally, we have identified an internal STS-marker, sTSG48370, which is located within the untranslated proportion of exon 8. The sirtuin catalytic domain, which is highly conserved in all members of mammalian sirtuins that have been described so far as well as in their Sir2 yeast ancestor protein, is found between amino-acid residues 52 and 221, i.e. within exons 2 and 7 of the protein (Fig. 3).

*Sirt6* is a single copy gene. Sequencing and results obtained by electronic PCR of BAC clone *RZPDB737G031026D6* identified STS-marker sTSG48370 to be located within the *Sirt6* genomic sequence. These data, together with the results obtained by electronic PCR and the reported location of the mentioned STS-markers, indicated one single site of hybridization of *Sirt6* on human metaphase chromosomes and its specific localization on chromosome 19p13.3 (Fig. 4).

*Sirt6* expression analyses. *In silico* expression profile analyses were carried out using the UniGene EST profile viewer, which is hosted by the NCBI homepage, and the Human GeneAtlas Gene Expression Database, which is hosted by the Genomics Institute of the Novartis Research Foundation (GNF) and which identified human SIRT6 to be most predominantly expressed in bone cells and in the ovaries but practically absent in bone marrow (39-42).

*Phylogenetic analysis and pairwise sequence comparisons.* We have screened the 'all non-redundant GenBank CDS translations + RefSeq Proteins + PDB + SwissProt + PIR + PRF expressed sequence tag database' ('nr' at NCBI) with



the human SIRT6 protein sequence and identified several yeast and human histone deacetylases which were sharing a significant degree of sequence homology with human SIRT6, indicating a high degree of phylogenetic conservation of protein structure and associated function throughout evolution. The tree was constructed after bootstrapping and depicts a subdivision into four main evolutionary branches (plants, insects, fish and mammals) (Fig. 5). In an additional analysis, a consensus evolutionary tree was obtained for class I through class IV human sirtuin and non-sirtuin HDACs on the basis of an alignment of the yeast RPD3, HDA1, SIR2 and HDAC11 human homologous proteins (Fig. 1). Obviously, the sirtuin family of HDACs (class III) does not reveal significant sequence homology with the three classes of non-sirtuin HDACs. The tree was constructed after bootstrapping and clearly identifies four families of human histone deacetylases with HDAC1, HDAC2, HDAC3 and HDAC8 being members of the yeast RPD3 family of histone deacetylases (so-called 'mammalian class I histone deacetylases'), HDAC4, HDAC5, HDAC6, HDAC7, HDAC9 and HDAC10 being members of the yeast HDA1 family of histone deacetylases (mammalian class II histone deacetylases) and SIRT1 through SIRT7 being homologs of the yeast SIR2 protein (mammalian class III histone deacetylases), while HDAC11 is so far the only member of a distinct group of class IV HDACs (Fig. 1) (4).

## Discussion

The human *Sirt6* gene encodes members of the sirtuin family of proteins which are referred to as class III NAD<sup>+</sup>-dependent histone deacetylases on the basis of their homology to the yeast Sir2 protein (5). The members of the sirtuin family are characterized by a sirtuin core domain and are grouped into four subclasses with SIRT6 being a class 4 sirtuin member (Fig. 1). For most of the currently known human sirtuins, a function has not yet been determined. In yeast, however, sirtuin proteins are known to regulate epigenetic gene silencing and suppress recombination of rDNA. In addition to their deacetylating activity, human sirtuins may function as intracellular regulatory proteins with mono-ADP-ribosyltransferase activity (2). Human *Sirt6* has been predicted to be predominantly a nuclear protein (30), which seems to be strongly expressed in bone cells and in the ovaries, while being practically absent in bone marrow (39-42). In the mouse embryo, SIRT6 has been reported to reach peak levels at day E11, which further persisted into adulthood in muscle, brain and heart cells (15).

In the present study, we report the identification, cloning and mapping of *Sirt6* on the genomic level. Human *Sirt6* is a single-copy gene that spans a region of approximately 8.5 kb. It is composed of 8 exons (Fig. 3 and Table II) ranging in size from 60 bp (exon 4) to 838 bp (exon 8) and reveals an accumulation of interspersed SINEs (Alu repeats) within introns 1, 3, and 4 (43). The SIR2 family domain is highly conserved within all members of mammalian sirtuin proteins that have been described so far and is located within exons 2 through 7 (Fig. 3). The 5' upstream *Sirt6* promoter region was found to contain a small 300 bp CpG island and lacks the canonical TATA- and CCAAT boxes (Fig. 2). TATA-

independent transcription in the presence of accumulated CpG elements has been described to be a typical feature of constitutively active housekeeping genes (44). Human *Sirt6* mRNA encodes a 355-aa protein with a predictive molecular weight of 39.1 kDa. Fluorescence *in situ* hybridization analysis in conjunction with electronic PCR localized the human *Sirt6* gene to the sub-band of chromosome 19p13.3 (Fig. 4), a region which has been found to be involved in numerous chromosomal abnormalities in association with malignant disease, especially in acute leukemias (403 of 522 cases) (Fig. 6). These data have been retrieved from the Cancer Genome Anatomy Project (CGAP) database at the National Cancer Institute (45).

It is currently not clear to what extent chromosomal abnormalities that involve the chromosome 19p13 chromosomal region have an influence on SIRT6-mediated functional effects. It is, however, evident that a number of sirtuin proteins are located within chromosomal regions that are particularly prone to chromosomal breaks. In such cases, gains and losses of chromosomal material may affect the availability of functionally active sirtuin proteins, which in turn disturbs the tightly controlled intracellular equilibrium of protein acetylation and/or ADP ribosylation, respectively (46). Protein acetylation modifiers are therefore gaining increasing attention as potential targets in the treatment of cancer. Relaxation of the chromatin fiber facilitates transcription and is regulated by two competing enzymatic activities, histone acetyltransferases (HATs) and histone deacetylases (HDACs), which modify the acetylation state of histone proteins and other promoter-bound transcription factors. While HATs, which are frequently part of multisubunit coactivator complexes, lead to the relaxation of chromatin structure and transcriptional activation, HDACs tend to associate with multisubunit corepressor complexes, which results in chromatin condensation and the transcriptional repression of specific target genes.

Unfortunately, it is currently not possible to assess to what extent human SIRT6 is playing a role in the pathogenesis of hematological malignancies and acute myeloid leukemia in particular. It is, however, evident that SIRT6 contains multiple repetitive elements at the genomic level, which makes the region particularly prone to chromosomal breaks, while it is located within a chromosomal region that is known to be frequently part of chromosomal alterations in acute leukemia. In the context of such chromosomal modifications that may involve SIRT6, the SIRT6 protein could potentially be either missing, dysfunctional or exhibit its enzymatic activity at wrong times in the wrong places and therefore contribute to an imbalance of the intracellular acetylation status and to the development of disease. The further characterization of the functional role of human SIRT6 is therefore likely to become an exciting endeavor.

## Acknowledgements

This work was supported by the German National Science Foundation (Deutsche Forschungsgemeinschaft, MA 2057/2-4).

## References

1. Frye RA: Phylogenetic classification of prokaryotic and eukaryotic Sir2-like proteins. *Biochem Biophys Res Commun* 273: 793-798, 2000.

2. Frye RA: Characterization of five human cDNAs with homology to the yeast SIR2 gene: Sir2-like proteins (sirtuins) metabolize NAD and may have protein ADP-ribosyltransferase activity. *Biochem Biophys Res Commun* 260: 273-279, 1999.
3. Brachmann CB, Sherman JM, Devine SE, Cameron EE, Pillus L and Boeke JD: The SIR2 gene family, conserved from bacteria to humans, functions in silencing, cell cycle progression, and chromosome stability. *Genes Dev* 9: 2888-2902, 1995.
4. Voelter-Mahlknecht S, Ho AD and Mahlknecht U: FISH-mapping and genomic organization of the NAD-dependent histone deacetylase gene, Sirtuin 2 (Sir2). *Int J Oncol* 27: 1187-1196, 2005.
5. Imai S, Armstrong CM, Kaerberlein M and Guarente L: Transcriptional silencing and longevity protein Sir2 is an NAD-dependent histone deacetylase. *Nature* 403: 795-800, 2000.
6. Vaquero A, Scher M, Lee D, Erdjument-Bromage H, Tempst P and Reinberg D: Human SirT1 interacts with histone H1 and promotes formation of facultative heterochromatin. *Mol Cell* 16: 93-105, 2004.
7. Blander G, Olejnik J, Krzymanska-Olejnik E, McDonagh T, Haigis M, Yaffe MB, *et al*: SIRT1 shows no substrate specificity *in vitro*. *J Biol Chem* 280: 9780-9785, 2005.
8. Blander G and Guarente L: The Sir2 family of protein deacetylases. *Annu Rev Biochem* 73: 417-435, 2004.
9. Straight AF, Shou W, Dowd GJ, Turck CW, Deshaies RJ, Johnson AD, *et al*: Net1, a Sir2-associated nucleolar protein required for rDNA silencing and nucleolar integrity. *Cell* 97: 245-256, 1999.
10. Fritze CE, Verschuere K, Strich R and Easton Esposito R: Direct evidence for SIR2 modulation of chromatin structure in yeast rDNA. *EMBO J* 16: 6495-6509, 1997.
11. San-Segundo PA and Roeder GS: Pch2 links chromatin silencing to meiotic checkpoint control. *Cell* 97: 313-324, 1999.
12. Kaerberlein M, McVey M and Guarente L: The SIR2/3/4 complex and SIR2 alone promote longevity in *Saccharomyces cerevisiae* by two different mechanisms. *Genes Dev* 13: 2570-2580, 1999.
13. Shore D, Squire M and Nasmyth KA: Characterization of two genes required for the position-effect control of yeast mating-type genes. *EMBO J* 3: 2817-2823, 1984.
14. Brunet A, Sweeney LB, Sturgill JF, Chua KF, Greer PL, Lin Y, *et al*: Stress-dependent regulation of FOXO transcription factors by the SIRT1 deacetylase. *Science* 303: 2011-2015, 2004.
15. Liszt G, Ford E, Kurtev M and Guarente L: Mouse Sir2 homolog SIRT6 is a nuclear ADP-ribosyltransferase. *J Biol Chem* 280: 21313-21320, 2005.
16. Sauve AA and Schramm VL: SIR2: the biochemical mechanism of NAD(+)-dependent protein deacetylation and ADP-ribosyl enzyme intermediates. *Curr Med Chem* 11: 807-826, 2004.
17. Tanny JC, Dowd GJ, Huang J, Hilz H and Moazed D: An enzymatic activity in the yeast Sir2 protein that is essential for gene silencing. *Cell* 99: 735-745, 1999.
18. Tanny JC and Moazed D: Coupling of histone deacetylation to NAD breakdown by the yeast silencing protein Sir2: evidence for acetyl transfer from substrate to an NAD breakdown product. *Proc Natl Acad Sci USA* 98: 415-420, 2001.
19. Tanner KG, Landry J, Sternglanz R and Denu JM: Silent information regulator 2 family of NAD-dependent histone/protein deacetylases generates a unique product, 1-O-acetyl-ADP-ribose. *Proc Natl Acad Sci USA* 97: 14178-14182, 2000.
20. Lin SJ, Kaerberlein M, Andalis AA, Sturtz LA, Defossez PA, Culotta VC, *et al*: Calorie restriction extends *Saccharomyces cerevisiae* lifespan by increasing respiration. *Nature* 418: 344-348, 2002.
21. Lin SJ, Defossez PA and Guarente L: Requirement of NAD and SIR2 for life-span extension by calorie restriction in *Saccharomyces cerevisiae*. *Science* 289: 2126-2128, 2000.
22. North BJ and Verdin E: Sirtuins: Sir2-related NAD-dependent protein deacetylases. *Genome Biol* 5: 224.1-7, 2004.
23. Motta MC, Divecha N, Lemieux M, Kamel C, Chen D, Gu W, *et al*: Mammalian SIRT1 represses forkhead transcription factors. *Cell* 116: 551-563, 2004.
24. Luo J, Nikolaev AY, Imai S, Chen D, Su F, Shiloh A, *et al*: Negative control of p53 by Sir2alpha promotes cell survival under stress. *Cell* 107: 137-148, 2001.
25. Vaziri H, Dessain SK, Ng Eaton E, Imai SI, Frye RA, Pandita TK, *et al*: hSIR2(SIRT1) functions as an NAD-dependent p53 deacetylase. *Cell* 107: 149-159, 2001.
26. Nemoto S, Fergusson MM and Finkel T: Nutrient availability regulates SIRT1 through a forkhead-dependent pathway. *Science* 306: 2105-2108, 2004.
27. Cohen HY, Miller C, Bitterman KJ, Wall NR, Hekking B, Kessler B, *et al*: Calorie restriction promotes mammalian cell survival by inducing the SIRT1 deacetylase. *Science* 305: 390-392, 2004.
28. Starai VJ, Celic I, Cole RN, Boeke JD and Escalante-Semerena JC: Sir2-dependent activation of acetyl-CoA synthetase by deacetylation of active lysine. *Science* 298: 2390-2392, 2002.
29. North BJ, Marshall BL, Borra MT, Denu JM and Verdin E: The human Sir2 ortholog, SIRT2, is an NAD(+)-dependent tubulin deacetylase. *Mol Cell* 11: 437-444, 2003.
30. Dryden SC, Nahhas FA, Nowak JE, Goustin AS and Tainsky MA: Role for human SIRT2 NAD-dependent deacetylase activity in control of mitotic exit in the cell cycle. *Mol Cell Biol* 23: 3173-3185, 2003.
31. Birnboim HC and Doly J: A rapid alkaline extraction procedure for screening recombinant plasmid DNA. *Nucleic Acids Res* 7: 1513-1523, 1979.
32. Mahlknecht U, Hoelzer D and Bucala R: Sequencing of genomic DNA. *Biotechniques* 27: 406-408, 1999.
33. Altschul SF, Madden TL, Schaffer AA, Zhang J, Zhang Z, Miller W, *et al*: Gapped BLAST and PSI-BLAST: a new generation of protein database search programs. *Nucleic Acids Res* 25: 3389-3402, 1997.
34. Wilbur WJ and Lipman DJ: Rapid similarity searches of nucleic acid and protein data banks. *Proc Natl Acad Sci USA* 80: 726-730, 1983.
35. Needleman SB and Wunsch CD: A general method applicable to the search for similarities in the amino acid sequence of two proteins. *J Mol Biol* 48: 443-453, 1970.
36. Thompson JD, Higgins DG and Gibson TJ: CLUSTAL W: improving the sensitivity of progressive multiple sequence alignment through sequence weighting, position-specific gap penalties and weight matrix choice. *Nucleic Acids Res* 22: 4673-4680, 1994.
37. Feng DF and Doolittle RF: Progressive sequence alignment as a prerequisite to correct phylogenetic trees. *J Mol Evol* 25: 351-360, 1987.
38. Fitzgerald M and Shenk T: The sequence 5'-AAUAAA-3' forms parts of the recognition site for polyadenylation of late SV40 mRNAs. *Cell* 24: 251-260, 1981.
39. Yang YH, Chen YH, Zhang CY, Nimmakayalu MA, Ward DC and Weissman S: Cloning and characterization of two mouse genes with homology to the yeast Sir2 gene. *Genomics* 69: 355-369, 2000.
40. Su AI, Cooke MP, Ching KA, Hakak Y, Walker JR, Wiltshire T, *et al*: Large-scale analysis of the human and mouse transcriptomes. *Proc Natl Acad Sci USA* 99: 4465-4470, 2002.
41. Su AI, Wiltshire T, Batalov S, Lapp H, Ching KA, Block D, *et al*: A gene atlas of the mouse and human protein-encoding transcriptomes. *Proc Natl Acad Sci USA* 101: 6062-6067, 2004.
42. Walker JR, Su AI, Self DW, Hogenesch JB, Lapp H, Maier R, Hoyer D and Bilbe G: Applications of a rat multiple tissue gene expression data set. *Genome Res* 14: 742-749, 2004.
43. Singer MF, Thayer RE, Grimaldi G, Lerman MI and Fanning TG: Homology between the KpnI primate and BamHI (M1F-1) rodent families of long interspersed repeated sequences. *Nucleic Acids Res* 11: 5739-5745, 1983.
44. Lewin B: Regulation of transcription. Oxford University Press, New York, 1997.
45. Mitelman F, Mertens F and Johansson B: A breakpoint map of recurrent chromosomal rearrangements in human neoplasia. *Nat Genet*: 417-474, 1997.
46. Mahlknecht U, Ottmann OG and Hoelzer D: When the band begins to play: Histone acetylation caught in the crossfire of gene control. *Mol Carcinog* 27: 268-271, 2000.